

# SEA LEVEL MONITORING USING A GNSS-BASED TIDE GAUGE

Johan S. Löfgren, Rüdiger Haas, Jan M. Johansson

Department of Radio and Space Science, Chalmers University of Technology, Onsala Space Observatory, SE-439 92 Onsala (Sweden), Email: johan.lofgren@chalmers.se, rudiger.haas@chalmers.se, jmj@chalmers.se

## ABSTRACT

A continuous monitoring of sea level changes is important for human society since more than 50% of the world's population live within 60 km of the coast. Sea level is traditionally observed with tide gauges that give measurements relative to the Earth's crust. To improve the understanding of sea level changes it is necessary to perform measurements with respect to the Earth's center of gravity. This can be done with satellite techniques, and thus a GNSS-based tide gauge is proposed that makes use of both GNSS-signals that are directly received and that are reflected on the sea surface. A test installation at the Onsala Space Observatory shows that the reflected GNSS-signals have only about 3 dB less signal-to-noise-ratio than the directly received GNSS-signals. A comparison of relative sea level observations from the GNSS-based tide gauge to traditional tide gauges gives an RMS-agreement on the order of 4 cm.

Key words: GNSS; reflection signals; sea level monitoring; tide gauge.

## 1. INTRODUCTION

Global climate change is believed to result in the melting of large masses of ice in Polar Regions, bringing freshwater into the ocean [1], and changing the sea level [2]. This can have important consequences for human society since more than 50% of the world's population live within 60 km of the coast [3]. The traditional way to measure the sea level, by tide gauges, results in measurements relative to the Earth's crust [4]. However, in order to fully understand sea level change processes, absolute measurements, i.e., change in sea level in relation to the Earth's center of gravity, are necessary. This is in particular important in regions that are affected by post-glacial uplift, e.g., Fennoscandia. Satellite techniques, e.g., Global Navigation Satellite Systems (GNSS), can be used to determine the motion of the Earth's crust in relation to the center of gravity [5]. By observing reflected GNSS-signals from the sea surface, information of both relative and absolute sea level change can be obtained. Therefore, a GNSS-based tide gauge is proposed.

## 2. INSTALLATION

The proposed GNSS-based tide gauge installation consists of two antennas, one zenith-looking right hand circular polarized (RHCP) and one nadir-looking left hand circular polarized (LHCP), mounted back-to-back on a beam over the ocean (see Fig. 1). The RHCP antenna receives the GNSS-signals directly, whereas the LHCP antenna receives the signals that are reflected from the sea surface. When the signals are reflected, they change polarization from RHCP to LHCP. The reflected signals experience an additional path delay, as compared to the directly received signals. This means that the LHCP antenna can be regarded as a virtual antenna located below the sea surface. This virtual antenna is depicted in blue in Fig. 1. When the sea level changes, the path delay of the reflected signal changes, thus the LHCP antenna will

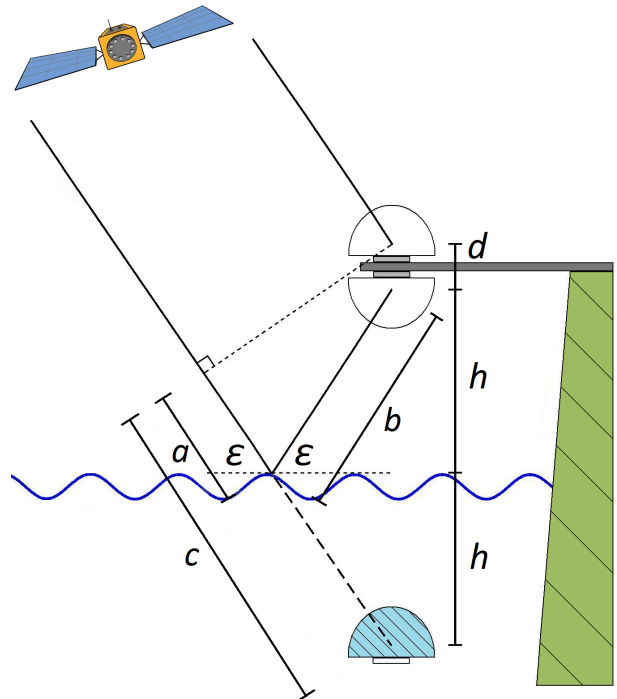


Figure 1. Schematic drawing of the GNSS-based tide gauge installation.

appear to change position. The vertical position change corresponds to twice the sea level change, which can be derived from the geometry in Fig. 1. The height of the LHCP antenna over the sea surface corresponds to

$$h = \frac{(a + b) / \sin \varepsilon - d}{2} \quad (1)$$

where  $a + b = c$  is the additional path delay of the reflected signal,  $\varepsilon$  is the elevation of the transmitting satellite, and  $d$  is the vertical separation between the phase centers of the RHCP and the LHCP antennas. A change in the sea level corresponds to a change in height for the LHCP antenna, thus the installation monitors sea level changes.

Multiple satellites with different elevation and azimuth angles are observed each epoch and will give rise to reflected signals with different incidence angles from different directions. This means that the estimated sea level change can not be considered to originate from one specific point on the sea surface, but rather represents the change of an average sea surface formed by the reflection points. The distribution of these points is limited by the placement of the antenna (height of the antenna, the landmass on which the antenna is positioned, and also obstacles in the water) and the antenna geometry.

### 3. EXPERIMENTAL SETUP AND EVALUATION

An experimental setup was installed in December 2008 over the ocean at the Onsala Space Observatory (OSO) at the west coast of Sweden, see Fig. 2. The antenna installation was mounted on the coastal bedrock so that there was open sea water in a southward direction. This was done in order to maximize the potential reflective surface. The downward looking LHCP antenna was approximately 1 m over the sea surface and both antennas were protected by hemispherical radomes.

Data were collected during three days using two Leica GRX1200+ receivers (one for the direct and one for the reflected signal) connected to one RHCP antenna (Leica AT504 GG choke-ring) and one LHCP antenna (Leica AR25 multi-GNSS choke-ring). The receivers recorded 40 hours of continuous Receiver Independent Exchange Format (RINEX) data [7] with 20 Hz sampling. The signal-to-noise ratio (SNR) as determined by the two receivers was used as a first data quality check. The receiver connected to the upward looking RHCP antenna received GNSS-signals from all direction except the north direction between  $-16^\circ$  and  $+6^\circ$  azimuth. The downward looking LHCP antenna received GNSS-signals from all directions except the north direction between  $-16^\circ$  and  $+22^\circ$  azimuth. The surrounding to the north of the GNSS-based tide gauge installation, between  $-135^\circ$  and  $+45^\circ$  azimuth, was dominated by bedrock from the coastline and a boathouse, while all other directions were open sea. The received signals in the north direction had low SNR compared to the rest of the signals, indicating influence of multipath reflections from the bedrock



Figure 2. The experimental setup of the GNSS-based tide gauge at Onsala Space Observatory.

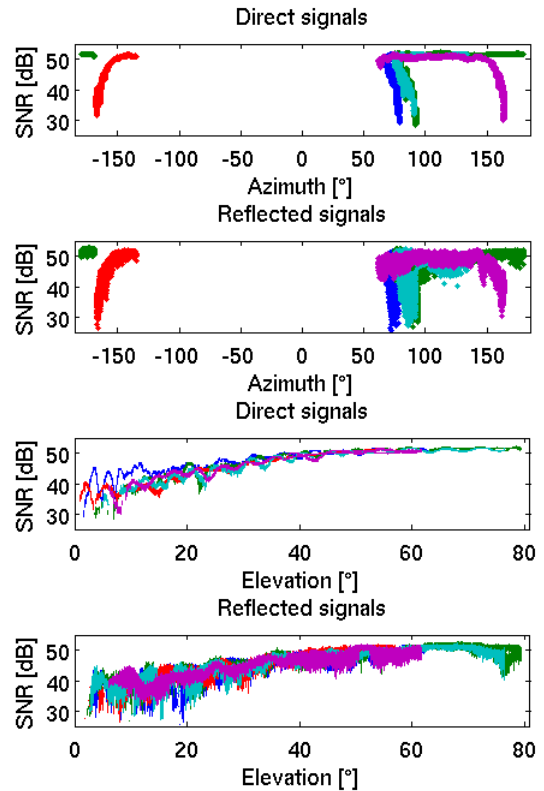


Figure 3. Signal-to-noise ratio, as determined by the two receivers, for the direct and reflected signals from 5 satellites during 4 hours as a function of azimuth (upper two panels) and elevation (lower two panels).

coastline and the boat house. To avoid influences of multipath we thus used an azimuth mask to excluded this region, and additionally applied an elevation mask of  $20^\circ$ . As an example Fig. 3 shows the SNR from both receivers for the remaining 5 satellites after the azimuth mask was applied. The satellites were continuously visible in the

south during 4 hours. In Fig. 3 it can be seen that the reflected signals are noisier than the direct signals (especially below  $20^\circ$  elevation). However, the SNR for the reflected signals is always above 25 dB and it increases with elevation.

In order to evaluate the average difference in SNR between the direct and the reflected signals, a second order polynomial was fitted to the SNR of each satellite arc. The differences between the SNR polynomials of the direct and the reflected signals were calculated for each satellite arc. In general, the SNR differences were larger for low elevations than for high elevations. The maximum SNR difference was 3.5 dB and this occurred for only one satellite at low elevations (less than  $20^\circ$  elevation). For all other satellites the SNR differences were less than 2.3 dB during the 4 hours.

#### 4. DATA ANALYSIS

The strategy to estimate the vertical difference between the RHCP and the LHCP antenna was to produce hourly estimates that could be compared to other data sets. First, to enable faster processing the 20 Hz data were decimated to 1 Hz data using the Translation, Editing, and Quality Check (TEQC) software [6]. Second, an elevation and azimuth mask for the installation site was applied, removing data below  $20^\circ$  elevation and outside the south direction  $-135^\circ$  to  $+45^\circ$  azimuth. This was done in order to remove unwanted signals, e.g., multipath from the coastline and to remove signals at low elevations. Reflected signals from low elevations have low SNR since they are highly elliptical polarized and at the Brewster angle even purely horizontal polarized [8].

Thereafter an in-house developed software in MATLAB was used to analyze the data. Solutions were made using L1 phase delays for relative positioning. Each solution used 20 minutes of data every full hour, solving for the difference in the local vertical component for this interval, together with receiver clock and phase ambiguity differences for each epoch (every second). The difference in local vertical component corresponds to  $2h + d$ , see Fig. 1. These results were used to calculate a time series of sea level  $h$ , and are presented in Fig. 4. The

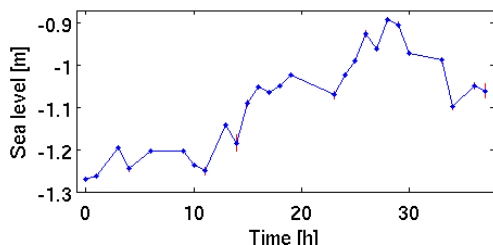


Figure 4. Sea level from the GNSS-based tide gauge during 40 hours. Values are relative to the RHCP antenna.

values shown in Fig. 4 are negative because they are relative to the upward looking RHCP antenna. Adding the ellipsoidal height of the RHCP antenna to these values will thus give absolute sea level heights in an ellipsoidal system.

#### 5. RESULTS

The resulting time series for the sea level change from the hourly solutions were compared to data from two traditional tide gauges operated by the Swedish Meteorological and Hydrological Institute (SMHI) at Ringhals and Göteborg, about 18 km south of and 33 km north of OSO, respectively (see Fig. 5). Since the sea level change from the GNSS-based tide gauge is relative to the position of the RHCP antenna, and the sea level changes of the traditional tide gauges refer to the mean sea level of the year, mean values were removed from each time series. This allows to compare the three series in a meaningful way avoiding any biases. The results are presented in Fig. 6.

To investigate the agreement of the three time series, the root-mean-square (RMS) differences were calculated. The RMS values are given in Tab. 1 and show that the agreement between the three independent time series is better than 4 cm. The traditional tide gauges appear to agree slightly better with respect to each other than the GNSS-based tide gauge to each of them. This indicates that there might still be some systematic effects that need further investigation.

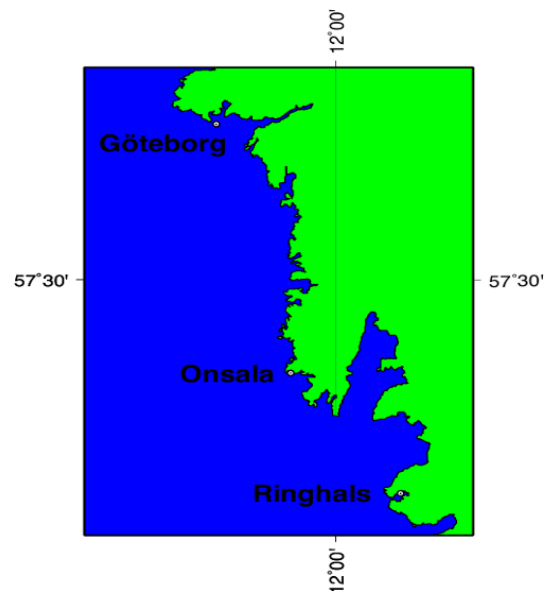


Figure 5. Map of parts of the Swedish west coast showing the locations of the traditional tide gauges at Göteborg and Ringhals, and the GNSS-based tide gauge at Onsala. The distances are about 33 km between Göteborg and Onsala, and 18 km between Onsala and Ringhals.

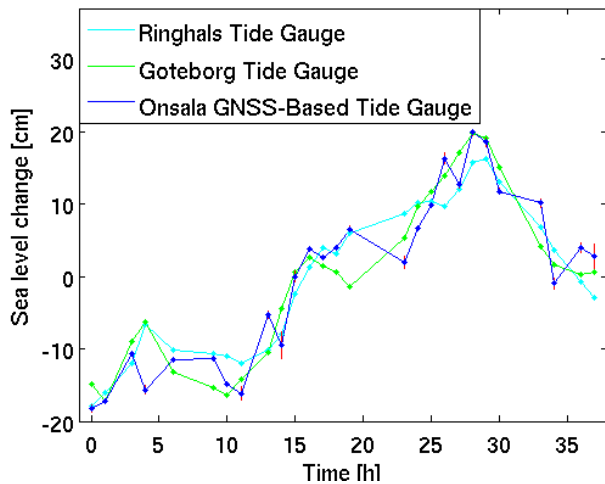


Figure 6. Sea level change from the GNSS-based tide gauge at OSO and from two traditional tide gauges at Ringhals and Göteborg. The mean is removed from each time series

Table 1. RMS-differences in sea level between tide gauges at Ringhals, Göteborg, and OSO.

Site 1	Site 2	RMS [cm]
Ringhals	OSO	3.7
Göteborg	OSO	3.7
Ringhals	Göteborg	3.3

## 6. CONCLUSIONS AND OUTLOOK

The GNSS-based tide gauge installation shows that it is possible to receive GNSS-signals reflected in the sea surface. As expected the reflected signals were noisier than the direct signals and the noise was higher at low elevations. The maximum reduction in SNR as compared to the directly received signals was 3.5 dB. However, the typically SNR difference was lower than 2.3 dB.

The GNSS-derived sea level change resembles reasonably well the independently observed sea level changes from two traditional tide gauges, and the RMS-agreement is better than 4 cm. The two traditional tide gauges agree slightly better than the GNSS-based tide gauge with each of them, indicating that there might be unaccounted systematic effects. One reason could be antenna phase center variations. The upward-looking RHCP antenna and the downward-looking LHCP antenna were two different types of antennas and phase center corrections were not applied to the data in the pre-processing. Another reason could be hydrodynamic effect differences due to the difference in geometry of the coast line at Ringhals, Onsala, and Göteborg.

The agreement between the GNSS-based tide gauge and the traditional tide gauges indicates that the GNSS-based tide gauge gives valuable results for sea level monitoring. Therefore, our plans are to install the GNSS-based tide gauge permanently at OSO during the fall of 2009. For this installation we plan to exchange the upward looking GNSS-antenna to an antenna of the same type as the downward looking one, but RHCP, in order to minimize systematic effects due to, e.g., phase center variation differences. Our ambition is to develop strategies for a real-time sea level monitoring with this installation.

Additionally, we plan to install a traditional tide gauge at the same site in order to further evaluate the GNSS-based tide gauge and to avoid any effects due to hydrodynamical differences caused by different coastal geometry.

Furthermore, we plan to analyze the high-rate (20 Hz) observations in post-processing. This high sampling rate might allow us to derive parameters that describe the sea surface roughness, as well as sea water properties.

## REFERENCES

- [1] Shum, C.K., Kuo, C.-Y., Braun A., Yi, Y. (2003). 20th Century Sea Level Rise. *Geophysical Research Abstracts*, Vol. 5, 07950.
- [2] Flather, R.A., Wakelin, S.L., Williams, J.A., Woodworth, P.L. (2003). Estimating effects of climate change on coastal sea levels. *Geophysical Research Abstracts*, Vol. 5, 12047.
- [3] United Nations Conference on environment and Development (1992). *Agenda 21*, Chapter 17.3.
- [4] Scherneck, H.-G., Johansson, J.M., Elgered, G., Davis, J.L., Jonsson, B., Hedling, G., Koivula, H., Ollikainen, M., Poutanen, M., Vermeer, M., Mitrovica, J.X., Milne, G. (2002). Bifrost: Observing the three-dimensional deformation of Fennoscandia. *Ice Sheets, Sea level and the Dynamic Earth, AGU Geodynamics Series 29*, 69-93, 10.1029/029GD05.
- [5] Johansson, J.M., Davis, J.L., Scherneck, H.-G., Milne, G.A., Vermeer, M., Mitrovica, J.X., Bennett, R.A., Jonsson, B., Elgered, G., Elsegui, P., Koivula, H., Poutanen, M., Rönnäng, B.O., Shapiro, I.I. (2002). Continuous GPS measurements of post-glacial adjustment in Fennoscandia 1. Geodetic results. *Journal of Geophysical Research*, Vol. 107, No. B8, 10.1029/2001JB000400.
- [6] Estey, L.H., Meertens, C.M. (1999). TEQC: The multi-purpose toolkit for GPS/GLONASS data. *GPS Solutions*, 3(1), 42-49.
- [7] Gurtner, W., Estey, L.H. (2005). RINEX: The Receiver Independent Exchange Format Version 2.11. <ftp://igsceb.jpl.nasa.gov/igsceb/data/format/rinex211.txt>
- [8] Hannah, B.M. (2001). Modelling and Simulation of GPS Multipath Propagation. *PhD thesis*, Queensland University of Technology.